Journal of Nuclear Medicine, published on February 23, 2018 as doi:10.2967/jnumed.117.204164

Impact of the AIF Recording Method on Kinetic Parameters in Small Animal PET

Hanna Napieczynska*[1,2], Armin Kolb*[1], Prateek Katiyar[1], Matteo Tonietto[3], Minhaz Ud-Dean[1], Ramona Stumm[1], Kristina Herfert[1], Carsten Calaminus[1], Bernd J. Pichler[1]

[1)] Werner Siemens Imaging Center, Department of Preclinical Imaging and Radiopharmacy, Eberhard Karls University Tuebingen, Tuebingen, Germany

[2)] International Max Planck Research School for Cognitive and Systems Neuroscience, Tuebingen, Germany

[3)] Institute for Brain and Spinal Cord, Sorbonne University, UPMC Univ Paris 06, Inserm U 1127, CNRS UMR 7225, Paris, France

* Authors contributed equally.

ABSTRACT

The goal of this study was to validate the use of a magnetic resonance-compatible blood sampler (BS) with the detector system based on lutetium oxyorthosilicate scintillator and avalanche photodiodes for small animal positron emission tomography (PET). **Methods:** Five rats underwent a 60 min ^{18}F-FDG study. For each animal, the arterial input function (AIF) was derived from the BS recording, from manual blood sampling (MS) and from the PET image. These AIFs were used for kinetic modelling of the striatum using the two tissue irreversible compartment model. The MS-based technique with a dispersion correction served as a reference approach and the kinetic parameters (KPs) estimated with the BS- and the image-derived (ID) AIFs were compared to the reference values. Additionally, the effect of applying a population-based plasma *versus* whole blood activity ratio $\left(\frac{p}{wb}\right)$ and the dispersion correction were assessed. **Results:** The K_1, k_2 and k_3 values estimated with the reference approach were 0.174±0.037 mL/min/cm^3, 0.342±0.080 1/min and 0.048±0.009 1/min, respectively. The corresponding parameters obtained with the BS- and ID-AIFs deviated from these values by 0.6-18.8 % and 16.7-47.9 %, respectively. To compensate for the error in the BS-based technique, data from one blood sample manually collected at the end of the experiment were combined with the data from the first 10 min of the BS recording. This approach allowed reducing the deviation in the KPs to 1.8-6.3 %. Using the $\frac{p}{wb}$ ratio led to the 1.7-8.3 % difference from the reference parameters. The sensitivity of the BS was 23 %, the energy resolution for the 511 keV photo peak was 19 % and the timing resolution was 11.2 ns. **Conclusions:** Online recording of the blood activity level with the BS allows precise measurement of the AIF, without losing the blood volume. Combining the BS data with one manually collected

blood sample is the most accurate approach for the data analysis. The high sensitivity of the device may allow applying lower radioactivity doses.

Key words: PET, blood sampler, arterial input function, kinetic modelling

INTRODUCTION

Small animal positron emission tomography (PET) provides a great opportunity to advance translational research in the field of molecular imaging. With the ultimate goal to develop specific and sensitive diagnostic tools for the patient's benefit, small animal studies focus on the development and characterization of new PET tracers and on investigating mechanisms of human diseases (*1,2*). An important aspect of all the preclinical studies is reliable and accurate quantification of the PET data (*3,4*).

Kinetic modelling allows reliable quantification (*5*) but it requires longer time for the acquisition of dynamic data. Moreover, recording of the arterial input function (AIF) is necessary if a reference region is not available. The AIF consists of the time activity curve (TAC) of the PET tracer level in the plasma (*p*) and in the whole blood (*wb*). The gold standard method of acquiring the AIF relies on manual blood sampling (MS). This, however, is challenging in small animals due to the loss of the blood volume which affects physiological stability (*6*).

Yet another difficulty is to accurately capture the peak activity after a bolus injection. Missing the peak may adversely influence the obtained kinetic parameters (KPs). Therefore, using a blood sampler (BS) with an arterial-venous shunt has been proposed (*6*). With this approach, the blood circulates in a closed system and the high sampling rate assures an accurate recording of the peak activity.

Although, several BSs have been described (*7-10*), only one currently available device (Twilite Two, Swisstrace, Zurich, Switzerland) is compatible with magnetic resonance imaging (MRI) scanners, enabling to record the AIF in PET/MRI studies (*11,12*). The compatibility is

achieved by separating the scintillation crystals from the photomultiplier tubes by a long optical fiber. However, this approach is known to degrade the PET signal due to a severe light loss by the optical fibers (*13*).

Alternatively, avalanche photodiodes, which are very compact and can be operated in the magnetic field, may replace photomultiplier tubes (*14*). Although the active area is smaller and the signal-to-noise ratio worse in avalanche photodiodes than in photomultiplier tubes, coupling them directly to cerium-doped lutetium oxyorthosilicate crystals compensates the signal-to-noise ratio, assuring high sensitivity (*15*).

A prototype BS with the avalanche photodiodes/lutetium oxyorthosilicate - based design has been developed for clinical PET/MRI applications (*15*). However, the dimensions of this device are not suitable for use in rodents. Therefore, the goal of our work was to build and test a similar BS, dedicated for small animal studies. Specifically, we used the BS to evaluate the impact of the AIF recording method on the KPs in rats. Moreover, the effect of applying a population-based *p versus wb* activity ratio $\left(\frac{\boldsymbol{p}}{\boldsymbol{wb}}\right)$ to calculate the AIF was assessed.

MATERIALS AND METHODS

Blood Sampler

The BS (Supplemental Fig. 1) was built based on the prototype device whose design and performance evaluation have been previously described (*15*). In the present device, two 3×4×5 cm^3 lutetium oxyorthosilicate blocks are attached to two 10×10 mm^2 avalanche photodiodes and a catheter is led between the detectors. Please, refer to the Supplemental Materials or contact the authors for more details regarding the device.

Nine calibration measurements ware carried out before the *in vivo* experiments. Firstly, the activity of ^{18}F-fluorodeoxyglucose (^{18}F-FDG) solution (3-4 MBq/1 mL) was measured in a well-counter (Capintec Inc., Pittsburgh, PA, USA). Subsequently, a 20 cm long catheter (low-density polyethylene, ID=0.4 mm, OD=0.8 mm, Reichelt Chemietechnik GmbH, Heidelberg, Germany), filled with this solution, was placed in the BS and the recording lasted 5-6 min. The sensitivity is expressed as the ratio of the measured mean count rate (corrected for the increased background of lutetium oxyorthosilicate crystals and for the decay) over the expected count rate.

The energy window for all the measurements was 350-1000 keV.

Animals

Animal procedures followed the standards of the care and use of laboratory animals and were approved by the local Animal Welfare and Ethics Committee of the Country Commission Tuebingen, Germany (Animal License No R2/16). Five Lister Hooded male rats (330-370 g, Charles River Laboratories, Wilmington, MA, USA) were kept in individually-ventilated cages

with free access to food and water until the time of the experiment. The temperature and humidity in the vivarium were 22±1 °C and 55±1 %, respectively.

Experimental Protocol

An isoflurane-oxygen mixture (CP-Pharma Handelsgesellschaft mbH, Burgdorf, Germany) was used for anesthesia (2.5 % for induction, 1.7 % for maintenance) and fentanyl for analgesia (Fentadon, Albrecht GmbH, Aulendorf, Germany, 5 µg/kg, *intraperitoneally*). A catheter (20 cm) was inserted into the tail vein and 1 mL of heparinized normal saline was administered.

Subsequently, a catheter was inserted into the right femoral artery for later MS, and the arterial-venous shunt into the contralateral femoral artery and vein. The shunt passed through the BS and a peristaltic pump (Ismatec REGLO-Digital, Cole-Parmer GmbH, Wertheim, Germany) (Supplemental Fig. 2), and it was composed of three pieces: arterial (40 cm), middle (30 cm), and venous (25 cm). The arterial and venous pieces, as well as the MS and the tail vein catheters, were made of the same tubing which was used for the sensitivity measurement. The middle piece was a Tygon tube (ID=0.44 mm, OD=2.26 mm, Ismatec). The pieces were joined by steel connectors (1.5 cm long, ID=0.3, OD=0.63 mm, Ismatec). The length from the arterial end of the shunt to the center of the BS field of view was the same as the length of the MS catheter (25 cm).

The body temperature was monitored with a rectal probe and the breathing rate visually every 15-20 min. ^{18}F-FDG in normal saline (54-75 MBq) was administered via the tail vein catheter with an infusion pump (0.5 mL over 25 s), which was directly followed by 0.1 mL of normal saline infused over 5 s. The pump, the BS recording, and the PET acquisition were started simultaneously. MS began 3 s earlier and continued until 75 s. Each sample of 3 blood drops (approximately 75 µL)

was collected in a capillary tube (Microvette CB 300 LH, Sarstedt, Nuembrecht, Germany). The number of the samples collected over that period was used to estimate the flow rate in the MS catheter. Subsequent samples were taken at: 3, 6, 10, 15, 25, 40, and 60 min. From each sample, 10 µL of the *wb* and 10 µL of the separated *p* (centrifugation: 4000 rpm, 5 min, 5 °C, 25 cm diameter) were measured with a γ-counter (2480 WIZARD^2, Perkin Elmer, Waltham, MA, USA).

At the end of the experiment, the venous piece of the shunt was cut and the blood flowing out was collected into two Eppendorf tubes, each time for 30 s. These volumes were measured to calculate the mean flow rate in the shunt. Finally, the animal was sacrificed with CO_2.

After each experiment, the BS was cross-calibrated with the well-counter. Moreover, the background activity was recorded and later subtracted from the BS dataset. The BS data were also decay-corrected.

PET

A small animal PET scanner (Inveon Dedicated PET, Siemens Healthineers, Knoxville, TN, USA) and Inveon Acquisition Workplace v.1.5.0.28 (Siemens Healthineers) were used for a 60 min PET acquisition, followed by a 10 min transmission scan performed with a rotating ^{57}Co source. The decay, dead time, and attenuation corrections, as well as normalization, were applied. The images were reconstructed with the filtered back-projection algorithm using the following framing: 18×5s, 1×30s, 3×60s, 1×180s, 1×120s, 1×300s, 3×900s, and subsequently analyzed with Pmod v.3.2 (PMOD Technologies LCC, Zürich, Switzerland). A volume of interest (24 mm^3) was drawn on the left ventricle (Supplemental Fig. 3) to obtain the image-derived (ID) AIF.

Delay and Dispersion

For each animal, the obtained *wb* MS- and BS-TACs were shifted on the time axis such that they overlaid with the first-above-baseline data point of the PET-TAC (Fig. 1). The average shift of the BS-TACs of the five rats was considered the delay of the system.

To estimate the dispersion factor, τ (*16*), an *in vitro* measurement based on the previously proposed design (*17*) was performed using human venous blood. This is described in the Supplemental Materials (Supplemental Figs. 4 and 5). The obtained τ was used to model the impulse response function of the system as a monoexponential function (*16*): $IRF = \frac{1}{\tau} exp\left(\frac{-t}{\tau}\right)$, where *t* is *time*. This was normalized to obtain a unit area under the curve (Supplemental Fig. 6) and the normalized impulse response function was used to deconvolve the MS- and BS-TACs, as described in the next section.

AIF

For each rat, the AIF was obtained in nine ways:

AIF FROM THE COLLECTED MANUAL SAMPLES ("MS"). The activity of the *wb* and *p* samples manually collected during the experiments was used as the AIF.

AIF FROM THE FITTED MANUAL SAMPLES ("MS-fit"). The original *wb* and *p* data were fitted using the previously described procedure (*18*) to remove the noise, which was necessary for the subsequent application of the dispersion correction. The obtained fits (wb_{MS-fit} and p_{MS-fit}) were used as the AIF to verify whether the fitting procedure itself would influence the KPs.

AIF FROM THE FITTED AND DISPERSION-CORRECTED MANUAL SAMPLES ("MS-fit-dc"). The normalized impulse response function was used to deconvolve the wb_{MS-fit} and the

p_{MS-fit} obtained previously. The outcome of the deconvolution ($wb_{MS-fit-dc}$ and $p_{MS-fit-dc}$) was used as the AIF. This approach was considered the reference throughout the study.

AIF FROM THE FITTED AND DISPERSION-CORRECTED MANUAL SAMPLES CALCULATED USING THE $\frac{p}{wb}$ *RATIO ("MS-fit-dc-calc").* A biexponential function has been shown to accurately describe the $\frac{p}{wb}$ for ^{18}F-FDG in rats (*6*). Hence, for each rat the ratio was first calculated using his original *p* and *wb* data:

$$\frac{p(t)}{wb(t)} = A * exp(-B * t) + C * exp(-D * t) + E$$

where *t* denotes *time* and *A*-*E* are the fit coefficients.

To avoid a strong weighting by the first 78 s data, when many samples were collected, only the first-above-baseline (*i.e.* >10 kBq/mL) and the last sample from this period were used (Fig. 2). Subsequently, the *A*-*E* coefficients of all five rats were averaged providing group mean values, A_m-E_m. These were: A_m = 0.418, B_m = 0.002, C_m = 0.214, D_m = 0.146, E_m = 1.245. They were used to calculate *p* values from the *wb* data:

$$p(t) = wb_{MS-fit-dc} * (A_m * exp(-B_m * t) + C_m * exp(-D_m * t) + E_m)$$

The $wb_{MS-fit-dc}$ and the calculated p values were used as the AIF. This procedure served to evaluate the effect of using the population-based $\frac{p}{wb}$.

AIF CALCULATED FROM THE BS DATA ("BS-calc"). The *p* values were calculated from the recorded *wb* BS data:

$$p(t) = wb_{BS} * (A_m * exp(-B_m * t) + C_m * exp(-D_m * t) + E_m)$$

The original wb_{BS} data and the calculated *p* values were used as the AIF.

AIF CALCULATED FROM THE FITTED BS DATA ("BS-fit-calc"). Analogically to the MS data, the wb_{BS} was fitted with the previously mentioned method (*18*). The obtained wb_{BS-fit} was used to calculate the *p* values:

$$p(t) = wb_{BS-fit} * (A_m * exp(-B_m * t) + C_m * exp(-D_m * t) + E_m)$$

The wb_{BS-fit} and the obtained *p* values were used as the AIF.

AIF CALCULATED FROM THE FITTED AND DISPERSION-CORRECTED BS DATA ("BS-fit-dc-calc"). The dispersion correction was applied to the wb_{BS-fit} in the same way as to the wb_{MS-fit}. The outcome ($wb_{BS-fit-dc}$) was subsequently used to calculate the *p* values:

$$p(t) = wb_{BS-fit-dc} * (A_m * exp(-B_m * t) + C_m * exp(-D_m * t) + E_m)$$

AIF DERIVED FROM THE PET IMAGE ("ID-calc"). The *wb* TAC from the left ventricle (wb_{PET}) was used to calculate the *p* values:

$$p(t) = wb_{PET} * (A_m * exp(-B_m * t) + C_m * exp(-D_m * t) + E_m)$$

The resultant *p* values and the wb_{PET} were used as the AIF.

AIF CALCULATED FROM THE FITTED AND DISEPRSION-CORRECTED COMBINATION OF THE BS AND MS DATA ("BSMS-fit-dc-calc"). The first 10 min of the BS recording was combined with one blood sample manually collected at 60 min. The combined data were fitted as previously (*18*) and the obtained $wb_{BSMS-fit}$ was corrected for dispersion ($wb_{BSMS-fit-dc}$). Then, the *p* values were calculated:

$$p(t) = wb_{BSMS-fit-dc} * (A_m * exp(-B_m * t) + C_m * exp(-D_m * t) + E_m)$$

Kinetic Modelling

Kinetic modelling of the right striatum (44 mm^3, Supplemental Fig. 7) was performed with Pmod. The two tissue compartment model assuming no dephosphorylation of FDG-6-phosphate ($k_4 = 0$) (*19*) was used. The blood volume in the brain was fixed at 5 %. Therefore, only K_1, k_2 and k_3, had to be estimated. No metabolite correction was applied. The estimated KPs were compared to the KPs obtained using the "MS-fit-dc" approach.

RESULTS

Performance of The System

The detection sensitivity of the BS was 23±1 % and the energy resolution was 19 % for the 511 keV photo peak with the timing resolution of 11.2 ns.

The flow rate was 1.2±0.4 mL/min in the MS catheter, and 1.2±0.1 mL/min in the shunt.

The delay in the shunt was 1.7±0.6 s. The mean dispersion coefficient, τ, assessed in the *in vitro* measurements was 1.94±0.38 (Supplemental Table 1).

Physiological Parameters

The temperature and the breathing rate were stable throughout the experiment (Supplemental Table 2). An example is shown in Fig. 3.

Whole Blood TACs

The *wb* MS-, BS-, and PET-TACs were in a good agreement. However, the PET-TAC was always the lowest in amplitude during the first 30 s. After approximately 10 min, it rose above the BS and MS values and this effect remained until the end of the measurement. Moreover, the BS-TAC tended to show slightly higher values than the MS-TAC in the second half of the experiment (Fig. 1).

The fitting procedure of the MS and of the BS data performed very well based on the visual inspection (Fig. 4).

Kinetic Modelling

The KPs estimated with the AIF obtained in nine different ways are presented in Table 1, Supplemental Table 3, and Supplemental Fig. 8. Using the original MS data as the AIF resulted in the K_1 value of 0.186±0.036 mL/min/cm^3 (mean±sd), the k_2 of 0.370±0.085 1/min, and the k_3 of 0.048±0.009 1/min. Fitting the AIF had only a small effect on the KPs, changing the K_1 to 0.179±0.039 mL/min/cm^3, the k_2 to 0.358±0.085 1/min, and the k_3 to 0.049±0.009 1/min. When the dispersion correction was applied, these values dropped by 2.9 %, 4.7 % and 2.1 %, respectively.

Using the $\frac{p}{wb}$ to obtain the AIF from the fitted and dispersion-corrected MS data resulted in an increase in the mean K_1 and k_2 by approximately 2 % compared to the reference values, while the mean k_3 rose by 8.3 %.

The mean K_1 and k_2 estimated with the AIF derived from the original BS data were comparable to the respective parameters obtained using the AIF from the original MS measures (0.189±0.030 mL/min/cm^3 and 0.350±0.057 1/min, respectively). However, the mean k_3 dropped by 14.6 %.

The AIF fitting procedure applied to the BS data had an even smaller effect than it had on the MS data. The mean K_1 did not change, while the mean k_2 and k_3 rose by 1.7 % and 2.1 %, respectively. Applying the dispersion-correction led to a reduction in the mean K_1, k_2 and k_3 by 3.4 %, 5.9 % and 6.3 %, respectively.

To correct for the discrepancy in the k_3 estimated with the “BS-fit-dc-calc” approach and the reference approach, the first 10 min of the BS recording were combined with one manually

collected sample, which was then fitted and dispersion-corrected to derive the AIF. The KPs estimated with this approach deviated from the respective reference values by only 1.8-6.3 %.

Finally, the differences between the mean KPs estimated with the ID-AIF and the reference KPs were 24.1 % for K_1, 16.7 % for the k_2, and -47.9 % for the k_3.

DISCUSSION

The present work demonstrates an implementation of the highly sensitive BS in a routine small animal PET study. Specifically, we used the device to evaluate the impact of differently acquired AIFs on the estimated KPs. Additionally, the effects of fitting the AIF, applying the dispersion correction, and using a population-based $\frac{p}{wb}$ activity ratio were evaluated.

The advantages of using the online BS shunt system with a high sampling rate in small animal PET include: an accurate capturing of the peak activity (*20*), avoiding blood loss which is not only crucial in mouse studies but very important even in rats (*6*), and avoiding removal of the PET tracer under investigation from the system while its level is being measured.

The BS used in this study provides additional benefits. The MR-compatibility allows for conducting simultaneous PET/MRI measurements which provide more detailed and complementary information about physiological processes (*2,12*). Furthermore, the very high sensitivity (23 %) may allow reducing the injected activity dose. Finally, using similar devices in preclinical and clinical experimental setups could facilitate translational research.

One limitation of using the BS recording is that the $\frac{p}{wb}$ radioactivity distribution over time needs to be known. This requires collecting manual samples, but can be done in a separate group of animals. Then, calculating the *p* activity from the BS data is based on the assumption that the ratio is the same in both groups. In our study, using the measured *p* values and the *p* values calculated from the manually collected *wb* samples with the group mean coefficients in the same animals resulted in the following deviations from the reference KPs: 1.7 % for K_1, 2.0 % for k_2,

and 8.3 % for k_3. These differences might be higher for a separate group of animals. Thus, if the population-based approach is used, it should be applied to all experimental groups.

Since the animals in our study were not fasted before the measurements, and the blood volume of 5 % was assumed for kinetic modelling (while 6 % may be more accurate (*21*), the obtained KPs may not be comparable with some results available in the literature. However, the main interest of the present work was to investigate the differences in the KPs of the five rats obtained using the AIFs acquired in different ways.

The *wb* TACs recoded by the BS were very similar to the ones measured by MS, especially right after the tracer administration. This was reflected in the very similar mean K_1 and k_2 in the MS- and BS-based estimates. The differences were in the 5 % range which still encompassed approximately 2 % deviation resulting from applying the $\frac{p}{wb}$ ratio. However, we observed an overestimation of the *wb* activity recorded by the BS compared to the MS method in the later stages of each measurement. This resulted in the underestimation of the k_3.

The overestimation in the BS-TAC was most probably caused by an adhesion of the blood to the inside walls of the shunt. Although this effect was not strong in our ^{18}F-FDG study and could be solved by combining the first 10 min of the BS data with only one manually collected sample, using a more lipophilic tracer might lead to larger deviations in the parameters which dependent mostly on the late phase of the recording. In those cases a polytetrafluoroethylene tubing could be used (*10*).

Additionally, despite heparinizing the animal, blocking of the blood flow in the shunt may sporadically occur, which also happened once in our study. In such a case, the shunt needs to be

opened and flushed, and the affected data should be removed from the analysis. Since blocking of the blood flow in the shunt is more probable in later phases of the experiment, it is beneficial if only the first 10 min of the BS recording is needed.

Although we did not apply sophisticated techniques for deriving the AIF from a PET image, a basic approach of this type was used for comparison. It resulted in high deviations of the KPs from the reference values, reaching almost 48 % for k_3. This is a known consequence of a gradual accumulation of ^{18}F-FDG in the myocardium and the subsequent spillover effect in the left ventricle (*22*). Additionally, due to the partial volume effect (*3*,*23*), the *wb* TAC was underestimated during the first minute of the acquisition leading to incorrect K_1 and k_2 values.

Although methods have been developed to correct for both the effects (*22*,*24*), and using iterative reconstruction algorithms could improve the image quality, a direct measurement of the radioactivity level in the blood remains the most reliable method. Moreover, in some studies the animal's heart may not be covered in the image which makes deriving the AIF impossible. This will be the case in studies utilizing a dedicated scanner for brain imaging (*25*). Therefore, an online radioactivity recording with a BS will remain an important tool in small animal PET.

CONCLUSION

We have established an experimental protocol for PET with an online radioactivity recording using the BS in rats. The acquired TACs closely resembled the TACs obtained by the gold standard MS method. Accordingly, the KPs estimated with the BS-derived AIF were in a good agreement with the reference values, although combining the first 10 min of the BS data with one manually collected sample provided the most accurate results.

Fitting the recorded AIF with the previously proposed method (*18*) allows correcting for the dispersion by the deconvolution with the impulse response function of the system. This fitting procedure has only a minor impact on the KPs. However, using the $\frac{p}{wb}$ activity ratio to obtain p values from the *wb* recording may have an effect on the KPs.

The exceptionally high sensitivity of the device (23 %) will be crucial for reducing radioactivity doses used in PET experiments and for studies utilizing short-lived isotopes.

FINANCIAL DISCLOSURE

This research received funding from the European Union Seventh Framework Program (FP7/2007-2013) under Grant Agreement No 602646 and from the German Research Foundation (PI 771/3-1).

ACKNOWLEDGEMENTS

We acknowledge Dr. Johannes Breuer, Dr. Geoffrey Warnock, Sandro Aidone, Prof. Adriaan Lammertsma and Dr. Masqsood Yaqub, and the Radiochemistry Group of the Werner Siemens Imaging Center.

REFERENCES

1. Vega SC, Weinl C, Calaminus C, et al. Characterization of a novel murine model for spontaneous hemorrhagic stroke using in vivo PET and MR multiparametric imaging. *NeuroImage.* 2017;155:245-256.

2. Maier FC, Wehrl HF, Schmid AM, et al. Longitudinal PET-MRI reveals [beta]-amyloid deposition and rCBF dynamics and connects vascular amyloidosis to quantitative loss of perfusion. *Nature medicine.* 2014;20:1485-1492.

3. Mannheim JG, Judenhofer MS, Schmid A, et al. Quantification accuracy and partial volume effect in dependence of the attenuation correction of a state-of-the-art small animal PET scanner. *PhysMed Biol.* 2012;57:3981-3993.

4. Mannheim JG, Schmid AM, Pichler BJ. Influence of Co-57 and CT Transmission measurements on the quantification accuracy and partial volume effect of a small animal PET scanner. *Mol Imaging Biol.* 2017;19:825-836.

5. Morris ED, Endres CJ, Schmidt KC, Christian BT, Muzic RF, Fisher RE. Kinetic modeling in positron emission tomography. In: Wernick MN, Aarsvold JN, eds. *Emission Tomography: The Fundamentals of PET and SPECT.* San Diego, CA: Academic; 2004:499-540.

6. Weber B, Burger C, Biro P, Buck A. A femoral arteriovenous shunt facilitates arterial whole blood sampling in animals. *Eur J Nucl Med Mol Imaging.* 2002;29:319-323.

7. Pain F, Laniece P, Mastrippolito R, et al. SIC, an intracerebral radiosensitive probe for in vivo neuropharmacology investigations in small laboratory animals: theoretical considerations and practical characteristics. *IEEE Trans Nucl Sci.* 2000;47:25-32.

8. Weber B, Späth N, Wyss M, et al. Quantitative cerebral blood flow measurements in the rat using a beta-probe and H215O. *J Cereb Blood Flow Metab.* 2003;23:1455-1460.

9. Alf MF, Wyss MT, Buck A, Weber B, Schibli R, Krämer SD. Quantification of brain glucose metabolism by 18F-FDG PET with real-time arterial and image-derived input function in mice. *J Nucl Med.* 2013;54:132-138.

10. Roehrbacher F, Bankstahl JP, Bankstahl M, et al. Development and performance test of an online blood sampling system for determination of the arterial input function in rats. *EJNMMI Phys.* 2015;2:1-19.

11. Warnock G, Özbay PS, Kuhn FP, et al. Reduction of BOLD interference in pseudo-continuous arterial spin labeling: towards quantitative fMRI. *J Cereb Blood Flow Metab.* 2017;0271678X17704785:1-10.

12. Wehrl HF, Wiehr S, Divine MR, et al. Preclinical and translational PET/MR imaging. *J Nucl Med.* 2014;55:11S-18S.

13. Shao Y, Cherry S, Farahani K, et al. Development of a PET detector system compatible with MRI/NMR systems. *IEEE Trans Nucl Sci.* 1997;44:1167-1171.

14. Pichler BJ, Judenhofer MS, Catana C, et al. Performance test of an LSO-APD detector in a 7-T MRI scanner for simultaneous PET/MRI. *J Nucl Med.* 2006;47:639-647.

15. Breuer J, Grazioso R, Zhang N, Schmand M, Wienhard K. Evaluation of an MR-compatible blood sampler for PET. *Phys Med Biol.* 2010;55:5883-5893.

16. Iida H, Kanno I, Miura S, Murakami M, Takahashi K, Uemura K. Error analysis of a quantitative cerebral blood flow measurement using H215O autoradiography and positron emission tomography, with respect to the dispersion of the input function. *J Cereb Blood Flow Metab.* 1986;6:536-545.

17. Munk OL, Keiding S, Bass L. A method to estimate dispersion in sampling catheters and to calculate dispersion-free blood time-activity curves. *Med Phys.* 2008;35:3471-3481.

18. Tonietto M, Rizzo G, Veronese M, Bertoldo A. Modelling arterial input functions in positron emission tomography dynamic studies. Paper presented at: Engineering in Medicine and Biology Society (EMBC), 2015 37th Annual International Conference of the IEEE, 2015.

19. Sokoloff L. Mapping cerebral functional activity with radioactive deoxyglucose. *Trends Neurosci.* 1978;1:75-79.

20. Ashworth S, Ranciar A, Bloomfield P. Development of an on-line blood detector system for PET studies in small animals. In: Myers R, Cunningham V, Bailey D, Terry J, eds. *Quantification of brain function using PET.* London, UK: Academic Press; 1996:62-66.

21. Lee HB, Blaufox MD. Blood volume in the rat. *J Nucl Med.* 1985;25:72-76.

22. Fang Y-HD, Muzic RF. Spillover and partial-volume correction for image-derived input functions for small-animal 18F-FDG PET studies. *J Nucl Med.* 2008;49:606-614.

23. Park M-J, Fung GS, Yamane T, Kaiser F, Fukushima K, Higuchi T. Assessment of partial volume effect in small animal cardiac PET imaging using Monte Carlo simulation. *J Nucl Med.* 2013;54:1638-1638.

24. Hsiao-Ming W, Sung-Cheng H, Allada V, Wolfenden PJ. Derivation of input function from FDG-PET studies in small hearts. *J Nucl Med.* 1996;37:1717-1722.

25. Yang Y, Bec J, Zhang M, et al. A high resolution prototype small-animal PET scanner dedicated to mouse brain imaging. *J Nucl Med.* 2016;115.165886:1-20.

FIGURES

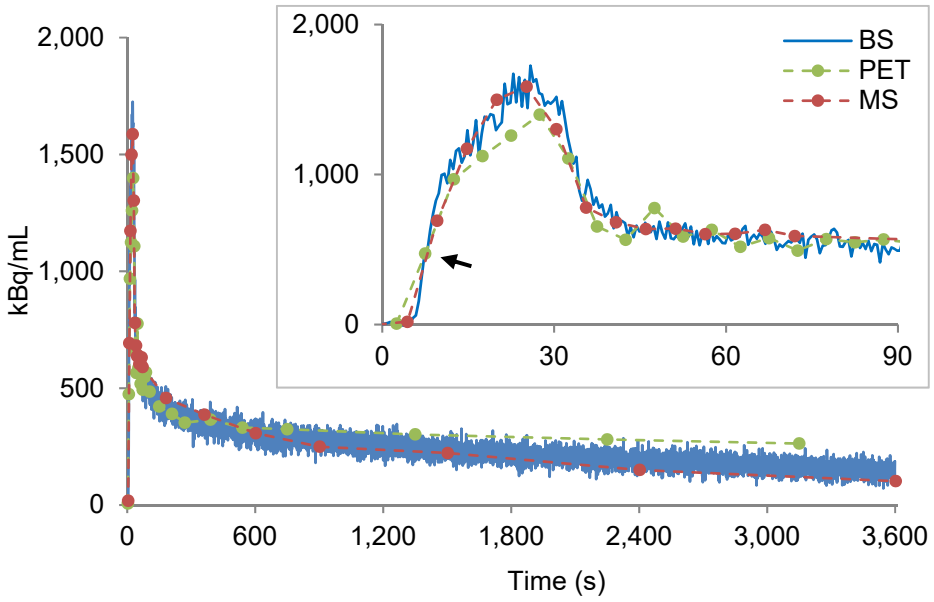

FIGURE 1. Example *wb* TACs Recorded by the BS, MS, and PET in One Rat. The MS- and BS-TACs were shifted on the time axis to match the first-above-baseline data point of the PET-TAC (arrow).

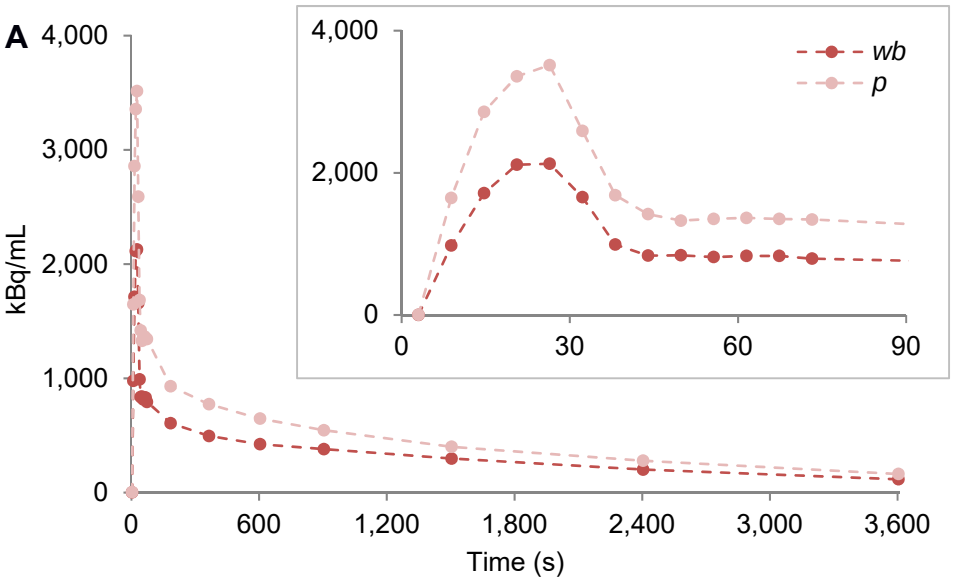

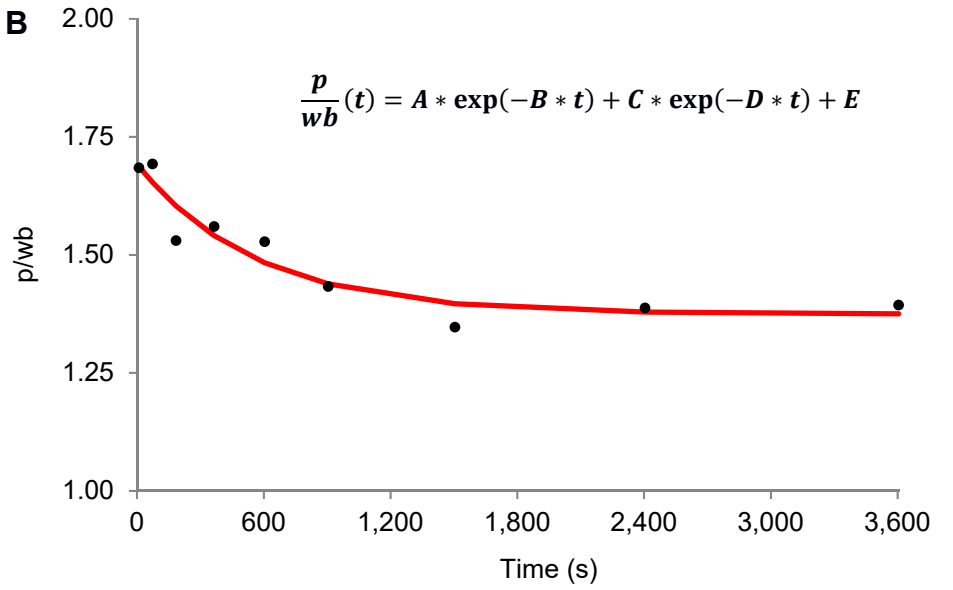

FIGURE 2. A. Example *wb* and *p* MS-TACs. **B.** The $\frac{p}{wb}$ ratio calculated from the samples shown in **A** (black dots) and the biexponential fit to these data (red line).

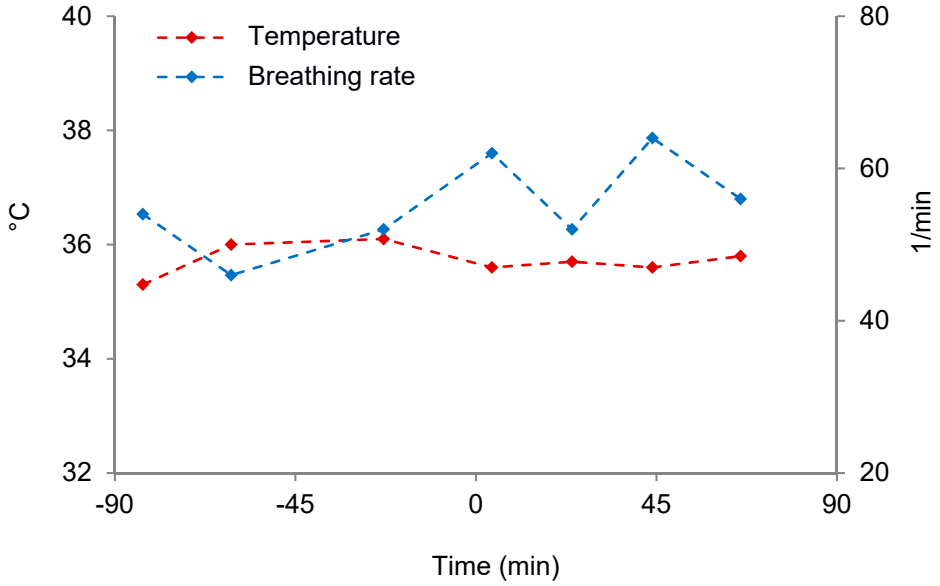

FIGURE 3. Physiological Parameters of One Rat.
The body temperature and the breathing rate were monitored from the moment of anaesthetizing the animal until the end of the experiment. “0 min” indicates the time point of the tracer injection.

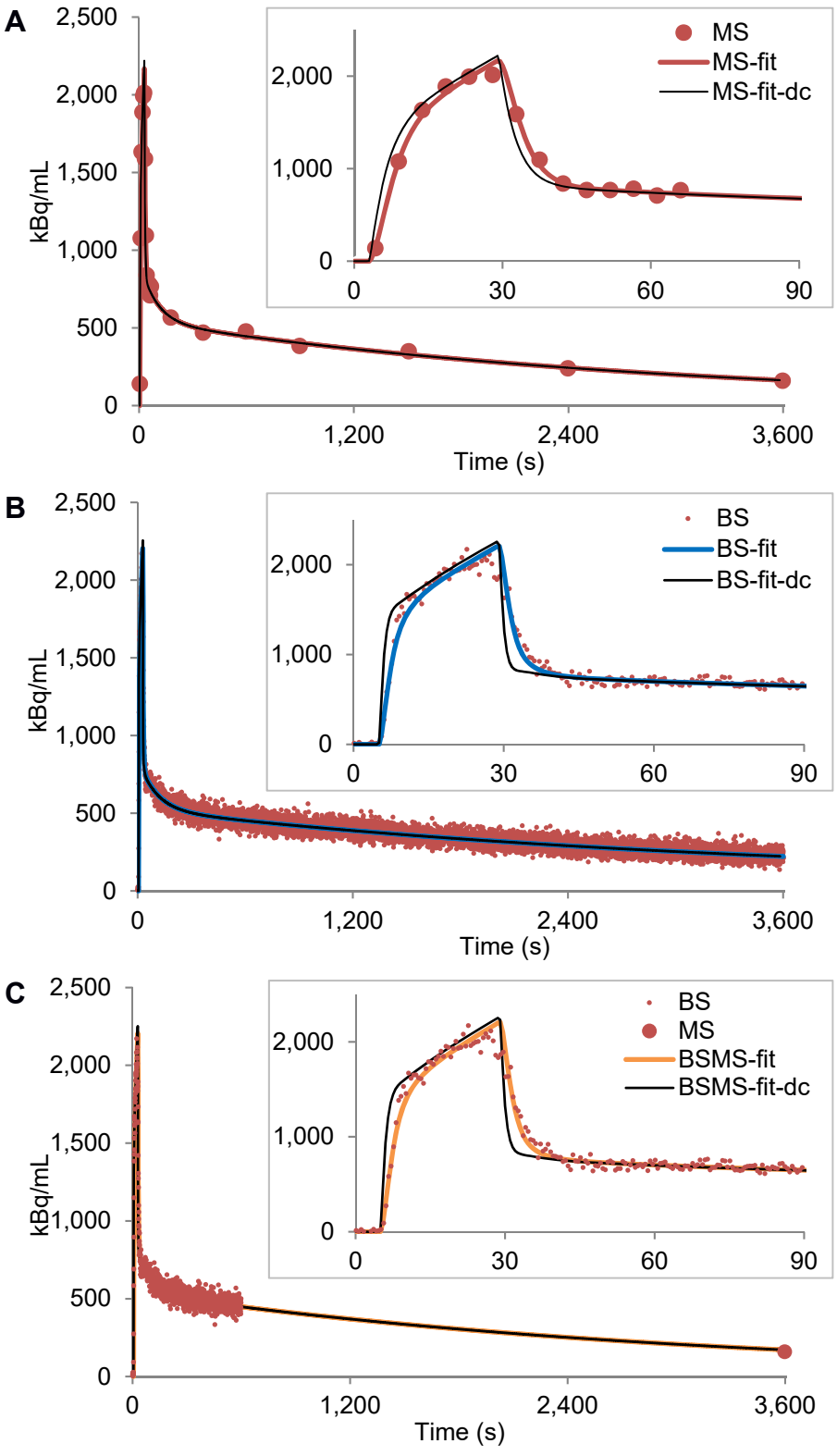

FIGURE 4. Fitting the *wb* TACs and Dispersion Correction. **A.** An exemplar *wb* TAC obtained by MS, a fit to that data (MS-fit) and the result of applying the dispersion correction (MS-fit-dc). **B.** The *wb* TAC recorded by the BS in the same animal, the fit to that data (BS-fit) and the dispersion-corrected fit (BS-fit-dc). **C.** The fitted combination of the BS and MS data (BSMS-fit) and the fit after applying the dispersion correction (BSMS-fit-dc).

TABLES

TABLE 1. The KPs were estimated using the AIF obtained in nine different ways. The AIF obtained from the fitted and dispersion-corrected manual samples (MS-fit-dc) was the reference approach. The mean ± sd of five rats is shown for K_1, k_2 and k_3. For each parameter, the % difference from the reference is shown in the neighboring column. Please, refer to the text for explanation of the abbreviations.

Method	K_1 (mL/min/cm^3)	% diff. from ref.	k_2 (1/min)	% diff. from ref.	k_3 (1/min)	% diff. from ref.
MS	0.186±0.036	6.9	0.370±0.085	8.2	0.048±0.009	0.0
MS-fit	0.179±0.039	2.9	0.358±0.085	4.7	0.049±0.009	2.1
MS-fit-dc (ref.)	0.174±0.037	0.0	0.342±0.080	0.0	0.048±0.009	0.0
MS-fit-dc-calc	0.177±0.031	1.7	0.349±0.071	2.0	0.052±0.010	8.3
BS-calc	0.189±0.030	8.6	0.350±0.057	2.3	0.041±0.010	-14.6
BS-fit-calc	0.189±0.028	8.6	0.344±0.047	0.6	0.042±0.007	-12.5
BS-fit-dc-calc	0.183±0.027	5.2	0.324±0.044	-5.3	0.039±0.008	-18.8
ID-calc	0.216±0.063	24.1	0.399±0.095	16.7	0.025±0.006	-47.9
BSMS-fit-dc-calc	0.185±0.028	6.3	0.336±0.047	-1.8	0.047±0.008	-2.1

Impact of the AIF Recording Method on Kinetic Parameters in Small Animal PET

Supplemental Materials

Hanna Napieczynska*[1,2], Armin Kolb*[1], Prateek Katiyar[1], Matteo Tonietto[3], Minhaz Ud-Dean[1], Ramona Stumm[1], Kristina Herfert[1], Carsten Calaminus[1], Bernd J. Pichler[1]

[1)] Werner Siemens Imaging Center, Department of Preclinical Imaging and Radiopharmacy, Eberhard Karls University Tuebingen, Germany

[2)] International Max Planck Research School for Cognitive and Systems Neuroscience, Tuebingen, Germany

[3)] Institute for Brain and Spinal Cord, Sorbonne University, UPMC Univ Paris 06, Inserm U 1127, CNRS UMR 7225, Paris, France

* Authors contributed equally.

1 MATERIALS AND METHODS

1.1 Blood Sampler

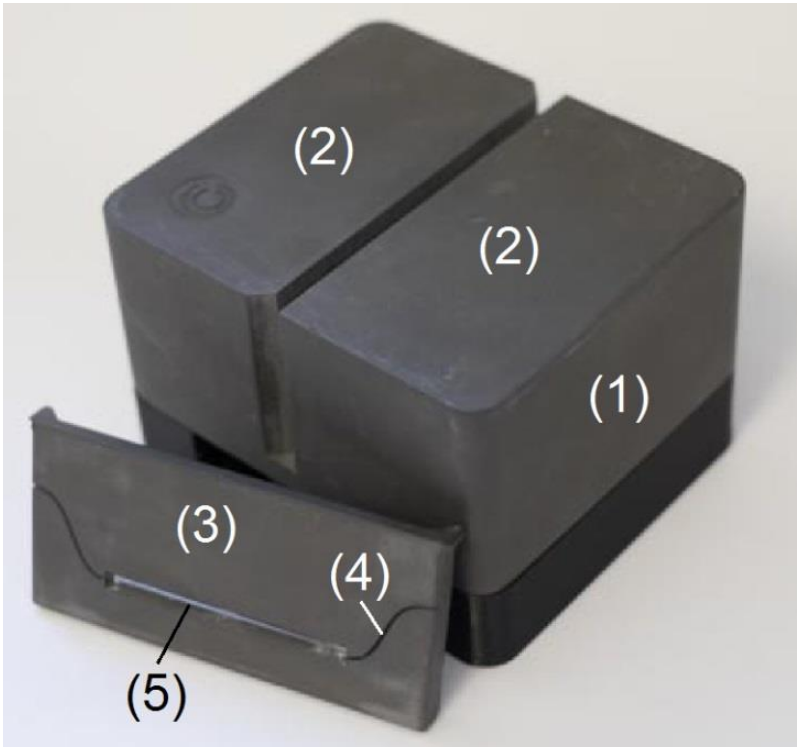

Supplemental Figure 1. Blood Sampler.
The 2.5 cm thick tungsten shielding (Tungsten Heavy Powder, San Diego, CA, USA) (1) has the density of 11 g/mm^3 and houses two LSO/APD detectors (2). They are separated with a removable cassette (3) made of the same material as the housing. The cassette has a groove for inserting the catheter (4) and a window (5) within which the activity is detected.
Each of the two APDs (S8664-1010, Hamamatsu, Japan) is characterized by the capacitance of 270 pF, the cut off frequency of 11 MHz, and the breakdown voltage of approximately 400 V. It is attached to a 3×4×5 cm^3 LSO block with a transparent silicone compound (RTV174). The LSO/APD detectors are orientated parallel to each other to provide a detection area of 4×5 cm^2. The crystals are molded into a housing made of a copper laminated composite material (FR-4) using the silicone compound previously combined with TiO_2 for an improved light collection. The compound also keeps the LSO blocks in a stable position which protects them from a mechanical damage.

1.2 Experimental Protocol

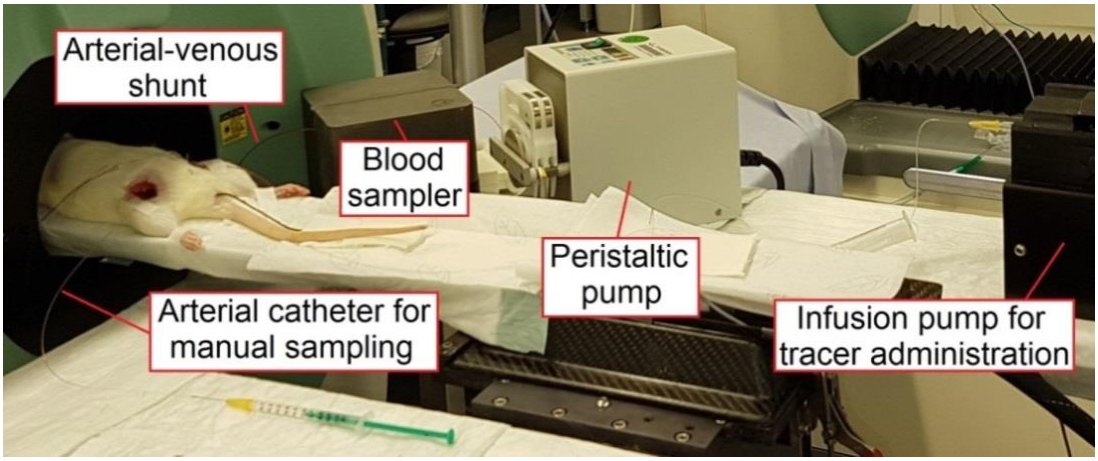

Supplemental Figure 2. Experimental Setup.
The arterial end of the shunt is inserted into the left femoral artery. After passing through the blood sampler and the peristaltic pump, the blood in the shunt returns to the animal's bloodstream via the venous end which is inserted into the femoral vein. The PET tracer is administered via the tail vein catheter with an infusion pump. Blood samples are manually collected from the right femoral artery. The body temperature is controlled with a rectal probe and maintained with a heating pad placed beneath the animal.

1.3 PET Measurements and Data Analysis

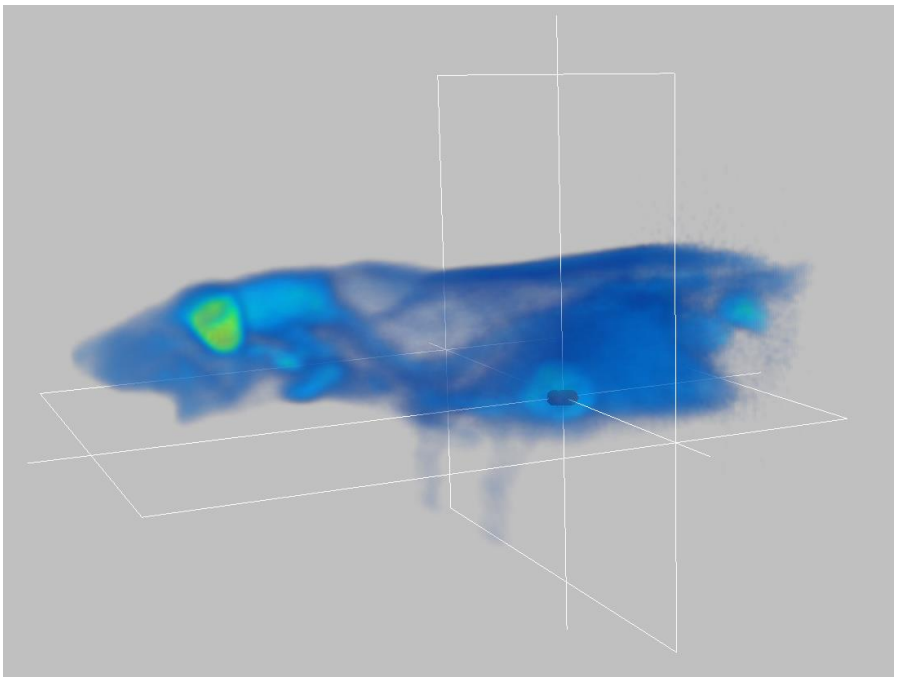

Supplemental Figure 3. Left Ventricle VOI.
The VOI (24 mm^3) was drawn on the ^{18}F-FDG PET image and is shown at the cross-section of the coronal and horizontal planes. The time activity curve from this VOI was used to obtain the image-derived arterial input function (ID-AIF).

1.4 Measurement of the Dispersion in the Shunt

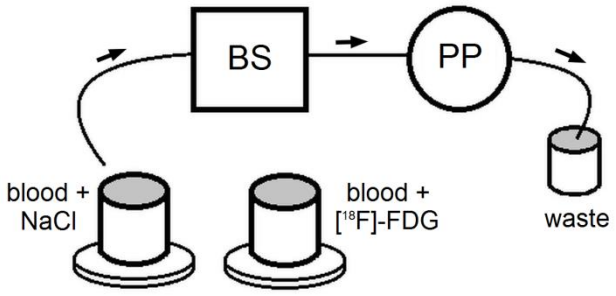

Supplemental Figure 4. Experimental Setup for the Measurement of the Dispersion.

The setup consisted of two cups with heparinized blood placed on magnetic stirring plates, the peristaltic pump (PP), the blood sampler (BS), and the catheter made of the same tubes which were later used in the *in vivo* measurements.

9.1 MBq of ^{18}F-FDG in 0.45 mL of normal saline was added to one of the cups and the same volume of normal saline to the second one. The pump was programmed as in the *in vivo* experiments. The "arterial" end of the tube was first dipped in the cup without the tracer to fill the entire length of the tube with blood. Then, the tube end was moved to the cup containing ^{18}F-FDG and kept there for approximately 1 min. This was followed by moving the tube end back to the first cup. Thus, a step function was recorded by the BS.

The pump was paused for about 2 s each time the cup was changed in order to avoid the air getting inside the tube. The entire procedure was repeated four times.

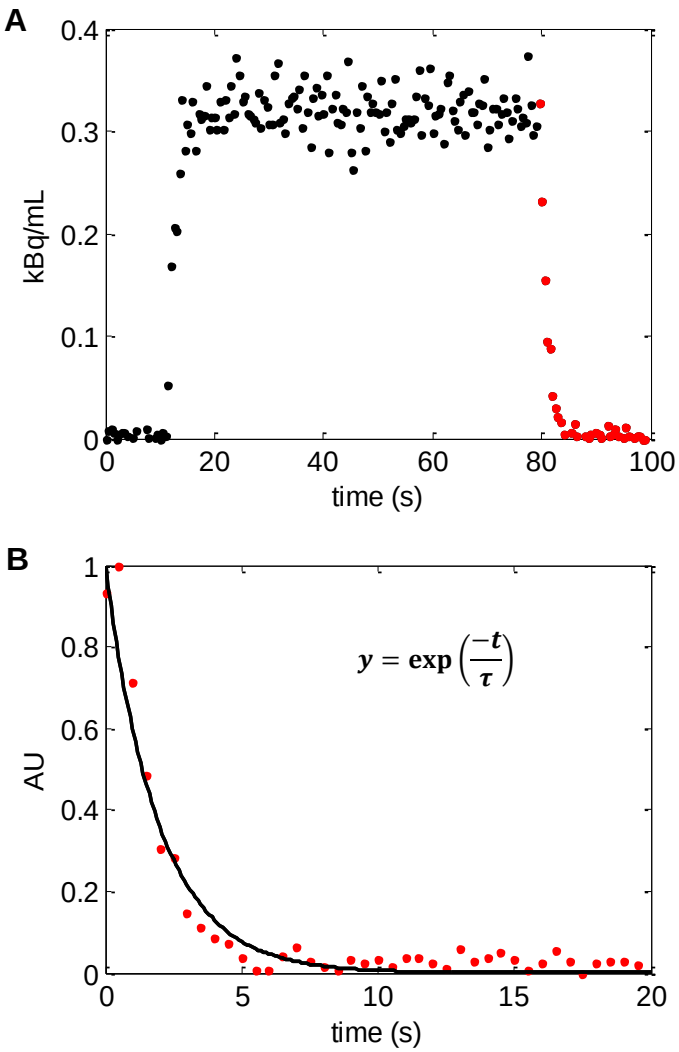

Supplemental Figure 5. Dispersion Factor.

A. An example step function recorded by the BS in the *in vitro* measurement after calibration and decay-correction.

B. The decaying portion of the "step" was normalized to 1 and a monoexponential fit was applied to estimate the dispersion factor, τ, according to (*17*). *t* denotes time.

The mean τ value of four measurements was considered the dispersion factor of the system.

1.5 Impulse Response Function (IRF)

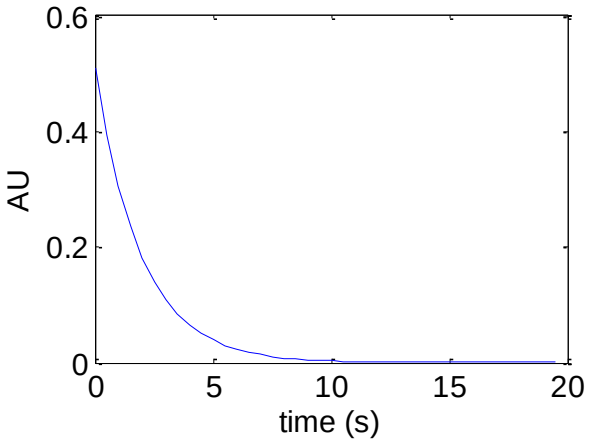

Supplemental Figure 6. The Normalized Impulse Response Function.

The normalized IRF was obtained with the mean dispersion factor, τ, and modelled as: $\boldsymbol{IRF} = \frac{1}{\tau}\exp\left(-\frac{t}{\tau}\right)$, according to (*17*). It was later used to deconvolve the fitted MS- and BS-TACs.

1.6 Kinetic Modelling

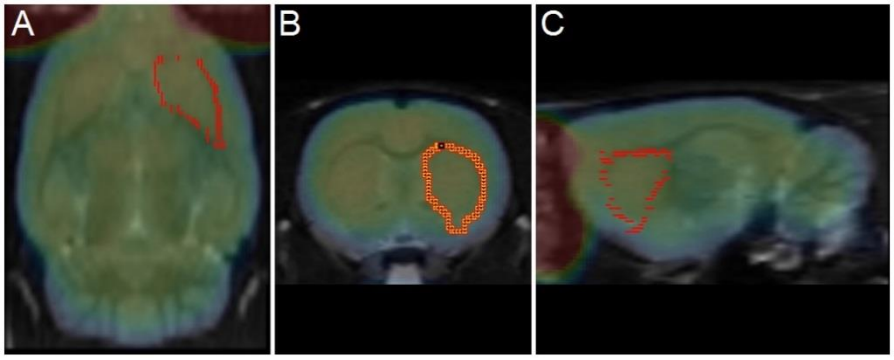

Supplemental Figure 7. The Right Striatum VOI.
The VOI is shown in the horizontal (**A**), coronal (**B**) and sagittal (**C**) plane. It was drawn on the MRI anatomical template provided in Pmod software, and copied onto the coregistered ^{18}F-FDG PET image to extract the TAC. The TAC was then used for kinetic modelling.

2 RESULTS

2.1 Dispersion

Supplemental Table 1. Dispersion Factor, τ.
It was estimated using a monoexponential fit to the decaying portion of the square step function (*17*) recorded by the BS *in vitro*. The measurement was repeated four times and the mean value was considered the dispersion factor of the system. The R^2 metric reflects the goodness of the fit.

Measurement	τ	R^2
1	1.51	0.97
2	1.96	0.95
3	2.43	0.93
4	1.86	0.95
Mean	**1.94**	
Sd	**0.38**	

2.2 Physiological Parameters

Supplemental Table 2. Physiological Parameters.
The breathing rate and the temperature were checked seven times throughout the duration of the experiment. The mean ± sd of these records for each rat is presented.

Rat	1	2	3	4	5
Breathing rate (1/min)	55±6	47±7	58±6	42±7	44±13
Temperature (°C)	35.7±0.3	35.1±0.6	35.6±0.8	35.3±0.6	35.5±0.4

2.3 Kinetic Modelling

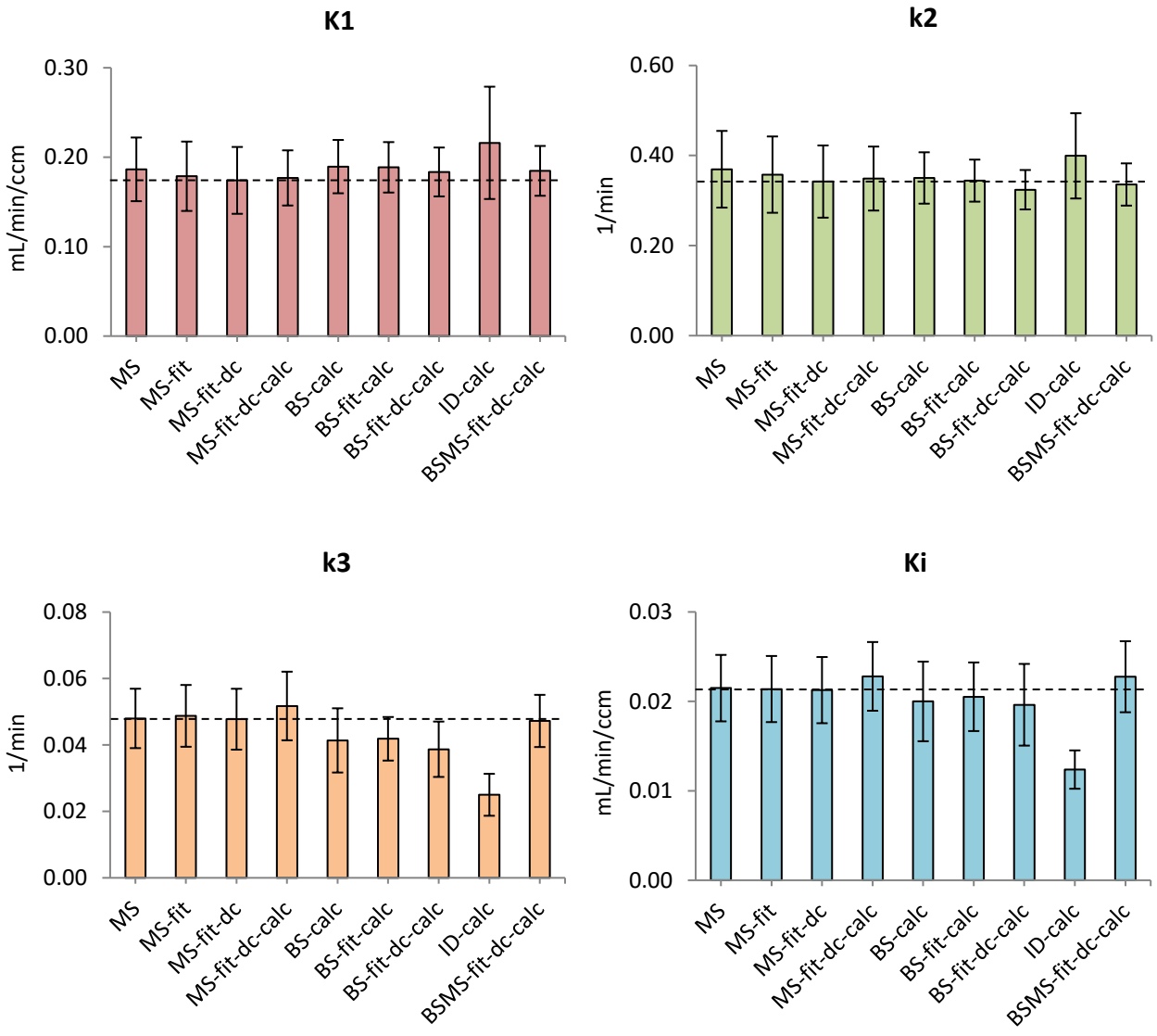

Supplemental Figure 8. Mean Kinetic Parameters.
The KPs were estimated using the AIF obtained in nine different ways (please, refer to the main text for explanation of the abbreviations). The bars represent mean ± sd of 5 rats. The AIF obtained from the fitted and dispersion-corrected manual samples (MS-fit-dc) was considered the reference approach (dashed line).

	MS				MS-fit				MS-fit-dc			
Rat	**K1**	**k2**	**k3**	**Ki**	**K1**	**k2**	**k3**	**Ki**	**K1**	**k2**	**k3**	**Ki**
1	0.139	0.256	0.044	0.020	0.123	0.245	0.045	0.019	0.120	0.236	0.044	0.019
2	0.182	0.374	0.049	0.021	0.181	0.370	0.054	0.023	0.175	0.352	0.053	0.023
3	0.171	0.343	0.035	0.016	0.170	0.331	0.035	0.016	0.166	0.318	0.034	0.016
4	0.232	0.493	0.059	0.025	0.230	0.481	0.059	0.025	0.224	0.459	0.058	0.025
5	0.208	0.381	0.052	0.025	0.190	0.361	0.051	0.024	0.185	0.347	0.050	0.023
average	**0.186**	**0.370**	**0.048**	**0.021**	**0.179**	**0.358**	**0.049**	**0.021**	**0.174**	**0.342**	**0.048**	**0.021**
sd	**0.036**	**0.085**	**0.009**	**0.004**	**0.039**	**0.085**	**0.009**	**0.004**	**0.037**	**0.080**	**0.009**	**0.004**
% diff from MS-fit-dc	6.9	8.2	0.0	0.0	2.9	4.7	2.1	0.0	0.0	0.0	0.0	0.0
	MS-fit-dc-calc				BS-calc				BS-fit-calc			
Rat	**K1**	**k2**	**k3**	**Ki**	**K1**	**k2**	**k3**	**Ki**	**K1**	**k2**	**k3**	**Ki**
1	0.136	0.255	0.045	0.021	0.152	0.284	0.034	0.016	0.154	0.300	0.033	0.015
2	0.183	0.382	0.057	0.024	0.180	0.329	0.042	0.020	0.177	0.300	0.038	0.020
3	0.166	0.316	0.037	0.017	0.180	0.331	0.029	0.015	0.182	0.363	0.041	0.019
4	0.221	0.445	0.062	0.027	0.232	0.437	0.053	0.025	0.229	0.411	0.050	0.025
5	0.178	0.348	0.057	0.025	0.203	0.370	0.048	0.024	0.201	0.348	0.046	0.024
average	**0.177**	**0.349**	**0.052**	**0.023**	**0.189**	**0.350**	**0.041**	**0.020**	**0.189**	**0.344**	**0.042**	**0.021**
sd	**0.031**	**0.071**	**0.010**	**0.004**	**0.030**	**0.057**	**0.010**	**0.004**	**0.028**	**0.047**	**0.007**	**0.004**
% diff from MS-fit-dc	1.7	2.0	8.3	9.5	8.6	2.3	-14.6	-4.8	8.6	0.6	-12.5	0.0
	BS-fit-dc-calc				ID-calc				BSMS-fit-dc-calc			
Rat	**K1**	**k2**	**k3**	**Ki**	**K1**	**k2**	**k3**	**Ki**	**K1**	**k2**	**k3**	**Ki**
1	0.150	0.288	0.033	0.015	0.208	0.348	0.029	0.016	0.150	0.288	0.047	0.021
2	0.172	0.285	0.037	0.020	0.194	0.320	0.022	0.013	0.174	0.307	0.049	0.024
3	0.177	0.322	0.029	0.015	0.221	0.392	0.019	0.010	0.178	0.334	0.035	0.017
4	0.223	0.393	0.049	0.025	0.315	0.562	0.021	0.011	0.225	0.411	0.057	0.027
5	0.196	0.332	0.045	0.023	0.143	0.375	0.034	0.012	0.197	0.339	0.048	0.025
average	**0.183**	**0.324**	**0.039**	**0.020**	**0.216**	**0.399**	**0.025**	**0.012**	**0.185**	**0.336**	**0.047**	**0.023**
sd	**0.027**	**0.044**	**0.008**	**0.005**	**0.063**	**0.095**	**0.006**	**0.002**	**0.028**	**0.047**	**0.008**	**0.004**
% diff from MS-fit-dc	5.2	-5.3	-18.8	-4.8	24.1	16.7	-47.9	-42.9	6.3	-1.8	-2.1	9.5

Supplemental Table 3. Individual Kinetic Parameters of Each Rat.

The KPs were estimated using the AIF obtained in nine different ways (please, refer to the main text for explanation of the abbreviations). The AIF obtained from the fitted and dispersion-corrected manual samples (MS-fit-dc) was considered the reference approach.